ISSN 0915-633X

NATIONAL INSTITUTE FOR FUSION SCIENCE

Period — 3 Catastrophe and Enhanced Diffusion in Two — Dimensional Hamiltonian Systems

Yoshi H. Ichikawa, Y. Nomura and T. Kamimura

(Received — Sept. 25, 1989)

NIFS-3 Jan. 1990

RESEARCH REPORT
NIFS Series

NAGOYA, JAPAN

Period - 3 Catastrophe and Enhanced Diffusion in Two - Dimensional Hamiltonian Systems

Yoshi H. Ichikawa, Y. Nomura and T. Kamimura

Abstract

Quantitative analysis of the period-3 catarophe is developed for the standard map and for the stochastic heating map as illustrative examples of two-dimensional area preserving mappings. Analtic expression of the diffusion coefficient is derived for the stochastic heating, and compared to results of numerical observation. Here, as for the case of the standard map, the multi-periodic accelerator modes give rise to anomalous enhancement of the diffusion rate.

Keywords :

period-3 catastrophe, standard map,

stochastic heating map, diffusion coefficient,

accelerator mode,

Poincare-Birkhoff period-q multifurcation,

squeeze effect, enhanced diffusion

1. Introduction

Stochasticity in the low dimensional Hamiltonian systems has been one of the central problems not only in the field of fundamental physics[1], but also under the light of practical interests of plasma confinement in the magnetic fusion devices[2][3], of plasma heating by the radio - frequency wave[4] and of the long time behaviour of particle beam in high energy accelerators[5][6]. Two-dimensional area-preserving mappings have been widely employed as a useful model of the nonlinear Hamiltonian systems. In a recent paper by Lichtenberg and Lieberman[7], calling ones attention to the fact that these model mappings can be smoothly transformed into dissipative mappings by variation of a parameter, they examined chaotic behaviour of both of the nonlinear conservative and dissipatibe systems. In order to explore statistical properties of the low dimensional Hamiltonian systems, we have been investigating various properties of the two-dimensional area-preserving maps in a series of papers[8]-[11].

Here, extending our analysis on the standard map, we want to discuss the period-3 catastrophe and enhanced diffusion in two-dimensional Hamiltonian systems. Summarizing our previous results obtained for the standard map, we discuss mechanism of the period-3 catastrophe in details in the next section. In order to illustrate the generic aspect of our analysis, we examine the stochastic heating of ions by the lower hybrid wave along the line of Karney's investigation[4] in the section 3 and 4. We present concluding discussions in the last section.

2. Period-3 Catastrophe in the Standard Map

The standard map,

$$P_{n+1} = P_n + \frac{A}{2\pi}\sin(2\pi X_n) \qquad [\mathrm{mod}\ 1]$$
$$X_{n+1} = X_n + P_{n+1} \qquad 1)$$

describes a dynamical system of particle motion under repetitive action of impulsive kicks, for which the Hamiltonian is given as

$$H = \frac{1}{2}P^2 - \frac{A}{2\pi}\cos(2\pi X)\sum_m \exp(i2\pi m\tau) \qquad 2)$$

Here, τ is a continuous time, normalized to the period of kicks. The remarkable properties of the standard map are its double periodicity in the action and phase variables.

The statistical property associated with the standard map is characterized by the diffusion coefficient of the action variable P,

$$D = \lim_{T\to\infty}\frac{1}{2T}\left\langle [P_T(i) - P_0(i)]^2 \right\rangle \qquad 3)$$

where the average < > is taken over the initial ensemble of i-th particles. Applying the Fourier path integral method, Meiss et al.[12] have derived an analytic expression for the diffusion coefficient eq.3) as

$$\frac{D}{D_Q} = \frac{1 - 2J_1^2(2\pi A) - J_2^2(2\pi A) + 2J_3^2(2\pi A)}{(1 + J_1(2\pi A))^2} \qquad 4)$$

where $J_n(x)$ is the n-th order Bessel function and $D_Q = A^2/4$. Comparing eq.4) with the observed diffusion coefficient in numerical experiments, we have identified that the enhanced deviation from the theoretical diffusion coefficient eq.4) is due to the multi-periodic accelerator modes. For the specific value of A $\approx$ 1.1, we have shown that the period-3 step-3 accelerator mode gives rise to the resonant enhancement of the diffusion.

Here, it may be worth to notice that Lichtenberg et al.[13] have measured stable area of the first accelerator mode of the standard map as a function of A, and identified the deep drop at A = $(6.95/2\pi)$ = 1.106 as the period-3 catastrophe. We should call ones attention to the similarity between Fig.1 of the referrence 12) and result obtained by Karney[14],(Fig.2 a) of the referrence 14)). Lichtenberg et al. noticed that the first dip at A $\approx$ $(6.62/2\pi)$ = 1.053 is due to the occurence of the period-4 step-4 accelerator mode (the 4:1 resonance).

Referring to symmetry structure of the standard map, we have examined the birth process of the period-q accelerator mode out of the first accelerator mode (the period-1 step-1 accelerator mode)[15]. Its threshould is given as

$$A(p/q) = \left\{ 1 + \frac{4}{\pi^2} \sin^4\left(\pi \frac{p}{q}\right)\right\}^{1/2} \qquad 5)$$

where p and q are the prime integers. For p=1, we have A(1/5) = 1.0238 and A(1/4) = 1.0494, which are consistent with our observation of birth of the period-5 and period-4 accelerator mode, respectively. Now, taking q=3 in eq.5), we get A(1/3) = 1.108, where we observed not the birth of the period-3 accelerator mode, but that the unstable period-3 accelerator mode squeezed to the origin. This is the phenomena called the period-3 catastrophe by Lichtenberg et al..

Determining explicitly the coordinates of the period-3 accelerator mode, we have identified the threshold of the onset of the period-3 accelerator modes as

$$A_0(1/3) = \left\{ 1 + \frac{2}{\pi^2} \right\}^{1/2} = 1.0967 \qquad 6)$$

while the squeezing condition of the unstaibe period-3 accelerator mode as

$$A_s(1/3) = \left\{ 1 + \left(\frac{3}{2\pi}\right)^2 \right\}^{1/2} = 1.1081 \qquad 7)$$

which is nothing but the value given by the Poincare-Birkhoff muiti-furcation condition, eq.5). Our analysis gives quantitative details of what Lichtenberg et al. called the period-3 catastrophe.

3. Stochastic Heating by the Lower Hybrid Wave

Stochastic heating of plasmas by radio-frequency wave has been regarded as one of the critical tool to heat confined plasmas in the magnetic fusion devices. Extending the early works of Fukuyama et al.[16] and Karney et al.[17], Karney[4] has examined throughly the process by introducing the two dimensional map

$$\begin{aligned} u_{j+1} &= u_j + 2\pi\delta - 2\pi A \cos v_j \\ v_{j+1} &= v_j + 2\pi\delta + 2\pi A \cos u_{j+1} \end{aligned} \qquad 8)$$

The Larmor radius of ions ρ is given by

$$\rho = \frac{1}{2}(v - u) \qquad 9)$$

and the phase of ion orbits θ is given by

$$\theta = \frac{1}{2}(v + u) \qquad 10)$$

Constructing a tangential map of eq.8), we can reduce the stability condition of fixed point or accelerator point at (u_0, v_0) as

$$A_l < A < A_u \qquad 11)$$

with

$$A_l \equiv \mathrm{Max}\left\{|m-\delta|, |n+\delta|\right\} \qquad 12)$$

and

$$A_u = \left[\frac{1}{2}\left\{(m-\delta)^2 + (n+\delta)^2 + \sqrt{\left((m-\delta)^2 - (n+\delta)^2\right)^2 + \frac{4}{\pi^4}}\right\}\right]^{1/2} \qquad 13)$$

The coordinates u_0 and v_0 are determined by

$$\delta + A\cos u_0 = m, \quad \delta - A\cos v_0 = -n \qquad 14)$$

with m and n the integers. Since we have

$$\rho_1 = \rho_0 + (m+n)\pi \qquad 15)$$

the point (u_0, v_0) with $m+n=0$ is the fixed point, while the point (u_0, v_0) with $m+n=1$ is the fundamental accelerator mode. The threshold of a Poincare-Birkhoff period-q multi-furcation around the point (u_0, v_0) is given by

$$A(p/q) = \left[\frac{1}{2}\left\{(m-\delta)^2 + (n+\delta)^2 + \sqrt{\left((m-\delta)^2 - (n+\delta)^2\right)^2 + \frac{4}{\pi^4}\sin^4\left(\pi\frac{p}{q}\right)}\right\}\right]^{1/2} \qquad 16)$$

with p and q the prime integers.

Now, the statistical properties of the heating process will be best characterized by the diffusion coefficient

$$D = \lim_{T\to\infty} \frac{1}{2T}\left\langle \left[\rho_T(i) - \rho_0(i)\right]^2 \right\rangle \qquad 17)$$

Approximate evaluations of eq.17) have been carried out by Antonsen et al.[18] and Karney et al.[19]. Here, we have carried out the renormalization analysis along the same lines of Meiss et al.[12], to obtain (setting $D_Q = \pi^2 A^2/2$)[20],

$$\frac{D}{D_Q} = \frac{1 - J_0^2(2\pi A)}{1 - 2J_0(2\pi A)\cos 2\pi\delta + J_0^2(2\pi A)} - \frac{4J_1^2(2\pi A)\cos 2\pi\delta}{\left[1 - 2J_0(2\pi A)\cos 2\pi\delta + J_0^2(2\pi A)\right]^2} \qquad 18)$$

We show the observed diffusion coefficient D for a value of $\delta = 0.47$ together with the anlytical result of eq.18) in Fig.1. We notice that for the value of $\delta = 0.47$, the first fixed point for (m=0, n=0) at $v_0 = \pm\cos^{-1}(\delta/A)$, $u_0 = \mp\cos^{-1}(\delta/A)+(2\ell+1)\pi$, with ℓ the integer, is stable in the region of

$$A_\ell = \delta = 0.47 < A < A_u = \sqrt{\delta^2 + \frac{1}{\pi^2}} = 0.5676 \quad 19)$$

while the second fixed point for (m=1, n=-1) at $v_0 = \pm\cos^{-1}(\delta-1/A)$, $u_0 = \mp\cos^{-1}(\delta-1/A)+(2\ell+1)\pi$, with ℓ the integer, is stable in the region of

$$A_\ell = 1-\delta = 0.53 < A < A_u = \sqrt{(1-\delta)^2 + \frac{1}{\pi^2}} = 0.6182 \quad 20)$$

As for the accelerator mode, the (m=1, n=0) mode and (m=0, n=-1) mode are stable in the region of

$$A_\ell^{(1)}(|s|=1) = 0.53 < A < A_u^{(1)}(|s|=1) = 0.597134 \quad 21)$$

and the (m=0, n=1) mode and (m=-1, n=0) mode are stable in the region of

$$A_\ell^{(2)}(|s|=1) = 1.47 < A < A_u^{(2)}(|s|=1) = 1.471794 \quad 22)$$

while the (m=2, n=-1) mode and (m=1, n=-2) mode are stable in the region

$$A_\ell^{(3)}(|s|=1) = 1.53 < A < A_u^{(3)}(|s|=1) = 1.531624 \quad 23)$$

Furthermore, having the step size $|s|=2$, the ($m=\pm1$, $n=\pm1$) modes are stable in the region of

$$A_\ell^{(1)}(|s|=2) = 1.47 < A < A_u^{(1)}(|s|=2) = 1.471851 \quad 24)$$

and the ($m=2$, $n=0$) mode and ($m=0$, $n=-2$) mode are stable in the region of

$$A_\ell^{(2)}(|s|=2) = 1.53 < A < A_u^{(2)}(|s|=2) = 1.531578 \quad 25)$$

while the ($m=0$, $n=2$) mode and ($m=-2$, $n=0$) mode are stable in the region of

$$A_\ell^{(3)}(|s|=2) = 2.47 < A < A_u^{(3)}(|s|=2) = 2.470353 \quad 26)$$

In Fig.1, we indicate the stable regions given by eqs.21),22),23),24), and 25) to show the enhancement of diffusion coefficient due to the presence of various accelerator modes.

4. Multi-periodic Accelerator Modes in the Stochastic Heating Map

Referring to our previous analysis of the diffusion process in the standard map, we expect that multi-periodic accelerator modes around the fundamental accelerator modes in the region of eq.21) are responsible for the enhancement of diffusion process observed in Fig.1.

Setting ($m=1$ and $n=0$) and ($m=0$ and $n=-1$) in eq.16), we obtain

$$\begin{aligned} A(\ 1/6\ ) &= 0.538668 \\ A(\ 1/5\ ) &= 0.544979 \\ A(\ 1/4\ ) &= 0.556576 \\ A(\ 1/3\ ) &= 0.576713 \\ A(\ 1/2\ ) &= 0.597134 \end{aligned} \qquad 27)$$

as the threshold of Poincare-Birkhoff period-q multifurcation around the fundamental accelerator modes located at

$$\begin{aligned} \rho_a &= \pm\frac{1}{2}\left[\cos^{-1}\frac{\delta-n}{A} + \cos^{-1}\frac{\delta-m}{A} - (2\ell+1)\pi\right] \\ \theta_a &= \pm\frac{1}{2}\left[\cos^{-1}\frac{\delta-n}{A} - \cos^{-1}\frac{\delta-m}{A} + (2\ell+1)\pi\right] \end{aligned} \qquad 28)$$

As for the onset of the period-6, period-5 and period-4 accelerator modes, our numerical observation confirms the values given in eq.27). With regard to the period-3 accelerator modes, however, we observe clearly the period-3 islands structure even at the smaller value of $A \sim 0.5740$ in Fig.2. Increasing the stochastic parameter upto the values of $A \sim 0.5760 \sim 0.5775$, we observe the squeezing effect in Fig.3.

In order to determine the exact values of the onset and the squeezing condition, we derive a reduced map around the accelerator mode at (u_a, v_a) by the following transformation.

$$\begin{aligned} x_j &= u_j - (u_a + 2\pi n j) \\ y_j &= v_j - (v_a - 2\pi m j) \end{aligned} \qquad 29)$$

Substitution of eq.29) into eq.8) gives rise to the reduced map

$$x_{j+1} = x_j + \alpha y_j + \beta y_j^2$$

$$y_{j+1} = y_j - \gamma x_{j+1} \tag{30}$$

with the abbreviations of

$$\alpha = 2\pi\sqrt{A^2 - (\delta + n)^2} \tag{31}$$

$$\beta = \pi(\delta + n) \tag{32}$$

$$\gamma = 2\pi\sqrt{A^2 - (\delta - n)^2} \tag{33}$$

Eq.30) determines one of the coordinates of the period-3 accelerator mode as

$$x_0 = 0 \tag{34}$$

$$y_0^{(\pm)} = \frac{1}{2\beta\gamma}\left\{2 - \alpha\gamma \pm \sqrt{(\alpha\gamma)^2 - 8}\right\} \tag{35}$$

where $y^{(+)}_0$ is the stable period-3 accelerator mode, while $y^{(-)}_0$ stands for the unstable period-3 accelerator mode.

Thus, the onset condition of the period-3 accelerator mode $(\alpha\gamma)^2 > 8$ determines

$$A_0(1/3) = \left[\frac{1}{2}\left\{(m-\delta)^2 + (n+\delta)^2 + \sqrt{\left((m-\delta)^2 - (n+\delta)^2\right)^2 + \frac{2}{\pi^4}}\right\}\right]^{1/2} \tag{36}$$

while the squeeze takes place when $y^{(-)}{}_0 \rightarrow 0$, so that a $\gamma = 3$ gives rise to

$$A_s(1/3)=\left[\frac{1}{2}\left\{(m-\delta)^2+(n+\delta)^2+\sqrt{\left((m-\delta)^2-(n+\delta)^2\right)^2+\frac{9}{4\pi^4}}\right\}\right]^{1/2} \qquad 37)$$

Taking $\delta = 0.47$ and (m=1 and n=0), eqs.36) and 37) determine, for the onset condition

$$A_0(1/3) = 0.573212 \qquad 38)$$

and for the squeeze condition

$$A_s(1/3) = 0.576713 \qquad 39)$$

respectively. Here, as was the case for the standard map, the squeeze condition for the period-3 accelerator mode eq.37) agrees eq.16) with $p/q = 1/3$.

To conclude the present section, we have carried out a detailed measurement of the diffusion coefficient in the range of $0.5<A<0.65$, where the presence of multi-periodic accelerator modes is expected to give rise to the enhanced diffusion. In order to avoid the direct contribution of the fundamental accelerator mode, we distribute 10^4 particles uniformly along the u axis, setting v=0, and we measure temporal evolution of the mean square average $\langle[p_T(i) - p_0(i)]^2\rangle$. Fig.4 shows the comparison between the theoretical curve of $g(A)=\sqrt{D/D_Q}$ given by eq.18) and observed results. In the sequence of the birth of period-

6 and period-5 accelerator mode, the diffusion coefficient grows over the theoretical curve and passes a dip in the course of growth of the period-4 accelerator mode and leads to a sharp dip before the onset of the period-3 accelerator mode. Here, it is very important to observe that even after the complete squeeze of the period-3 the observed diffusion coefficient exceeds over the analytical values over a wide range of the stochastic parameter.

5. Concluding Discussions

Here, referring to our analysis on the standard map, we have given quantitative analysis of the period-3 catastrophe in the two dimensional area preserving map with the accelerator modes. Statistical properties of the stochastic heating map have been examined in details. Both of the standard map and the stochastic heating map confirm that the multi-periodic accelerator modes give rise to the large enhanced peaks in the diffusion coefficient. As for the stochastic heating map, even after the squeeze of the period-3 accelerator mode is completed the reminiscent of the stable period-3 accelerator mode gives rise to the enhancement over the analytic prediction.

In this regard, it will be worth to remark that Mori and his collaborators extended their analysis of the q-phase transition method[21] to the conservative system[22], and found that the contribution of the period-3 accelerator mode exhibits clear q-phase transition associated, while the transition associated with the higher periodic accelerator modes is not observed. It would be important to examine this aspect to explore the physical process associated with the so called period-3 catastrophe.

Acknowledgement

The part of this paper was presented at the US-Japan Workshop on Low Dimensional Nonlinear Dynamics and Applications to Plasma Physics, held at Boulder, Colorado during July 24 - 28, 1989. The authors oblidged to Professors A.J.Lichtenberg and J.R.Cary for their stimulating discussions.

It is our great pleasure to dedicate this paper to Professor Hazime Mori on the occasion of his retirement from Kyusyu university.

Referrences

1) A.J.Lichtenberg and M.A.Lieberman, Regular and Stochastic Motion (Springer, New York, 1983)

2) J.M.Greene, Statistical Physics and Chaos in Fusion Plasmas, C.W. Horton and L.E.Reichl, eds. (John Wiley, New York, 1984) p.3

3) R.B.White, ibid, p.209

4) C.F.F.Karney, Phys.Fluids 22(1979)2188

5) See for instance, Nonlinear Dynamics Aspects of Particle Accelerators, Lecture Notes in Physics, Vol.247 (Springer, Berlin, 1986)

6) R.L.Warnock and R.D.Ruth, Physics 26D(1987)1

7) A.J.Lichtenberg and M.A.Lieberman, Physica 33D(1988)211

8) Y.H.Ichikawa, T.Kamimura, and C.F.F.Karney, Physica 6D(1983)233

9) Y.H.Ichikawa, T.Kamimura, and T.Hatori, Statistical Physics and Chaos in Fusion Plasmas, C.W.Horton and L.E.Reichl,eds.(John Wiley, New York, 1984)p.21

10) T.Hatori, T.Kamimura, and Y.H.Ichikawa, Physica 14D(1985)193

11) Y.H.Ichikawa, T.Kamimura, and T.Hatori, Physica 29D(1987)247

12) J.D.Meiss, J.R.Cary, C.Grebogi, J.D.Crawford, A.N.Kaufman and H.D.I. Abarbanel, Physica 6D(1983)375

13) A.J.Lichtenberg, M.A.Lieberman and N.W.Murray, Physica 28D(1987) 371

14) C.F.F.Karney, Physica 8D(1983)360

15) Y.H.Ichikawa, T.Kamimura, T.Hatori and S.Y.Kim, Suppl.Prog.Theor. (to be pubished)

16) A.Fukuyama, H.Momota, R.Itatani and T.Tokizuka, Phys.Rev.Lett.38 (1977)701

17) C.F.F.Karney and A.Bers, Phys.Rev.Lett.39(1977)550

18) T.M.Antonsen, Jr. and E.Ott, Phys.Fluids.24(1981)1635

19) C.F.F.Karney, A.B.Rechester, and R.B.White, Physica 4D(1982)425

20) Y.Nomura, Kakuyugo Kenkyu 62(1989) (to be published)

21) H.Hata, T.Horita, H.Mori, T.Morita and K.Tomita, Prog.Theor. Phys. 81(1989)11

22) H.Mori, Bifurcations of Chaos and q-phase Transitions, Report in the US-Japan Workshop on Low-Dimensional Nonlinear Dynamics and Applications to Plasma Physics, held at Boulder, Colorado, July 24 -28, 1989

Captions of Figures

Fig.1 The normalized diffusion rate D/D_0 for various values of A in the stochastic heating map for the value of $\delta=0.47$. The thin curve represents the theoretical diffusion rate of eq.18). The black circles represent results of our measurement, while the crosses are taken from Fig.9 of the referrence 4. The shaded region stands for eq.21), the vertical line at $A\approx1.47$ stands for eqs.22) and 24) and the vertical line at $A\approx1.53$ stands for eq.23) and 25)

Fig.2 The period-3 accelerator modes at $A=0.5740$ for $\delta=0.47$.

Fig.3 Squeezing of the period-3 accelerator modes at $A=0.5770$ for $\delta=0.47$

Fig.4 The square root $g(A)$ of the normalized diffusion rate D/D_0 as a function of A for the value of $\delta=0.47$. The vertical lines indicate positions of the onset of designated periodic accelerator modes. The broken vertical line indicates the value of A squeezing of the period-3 accelerater takes place.

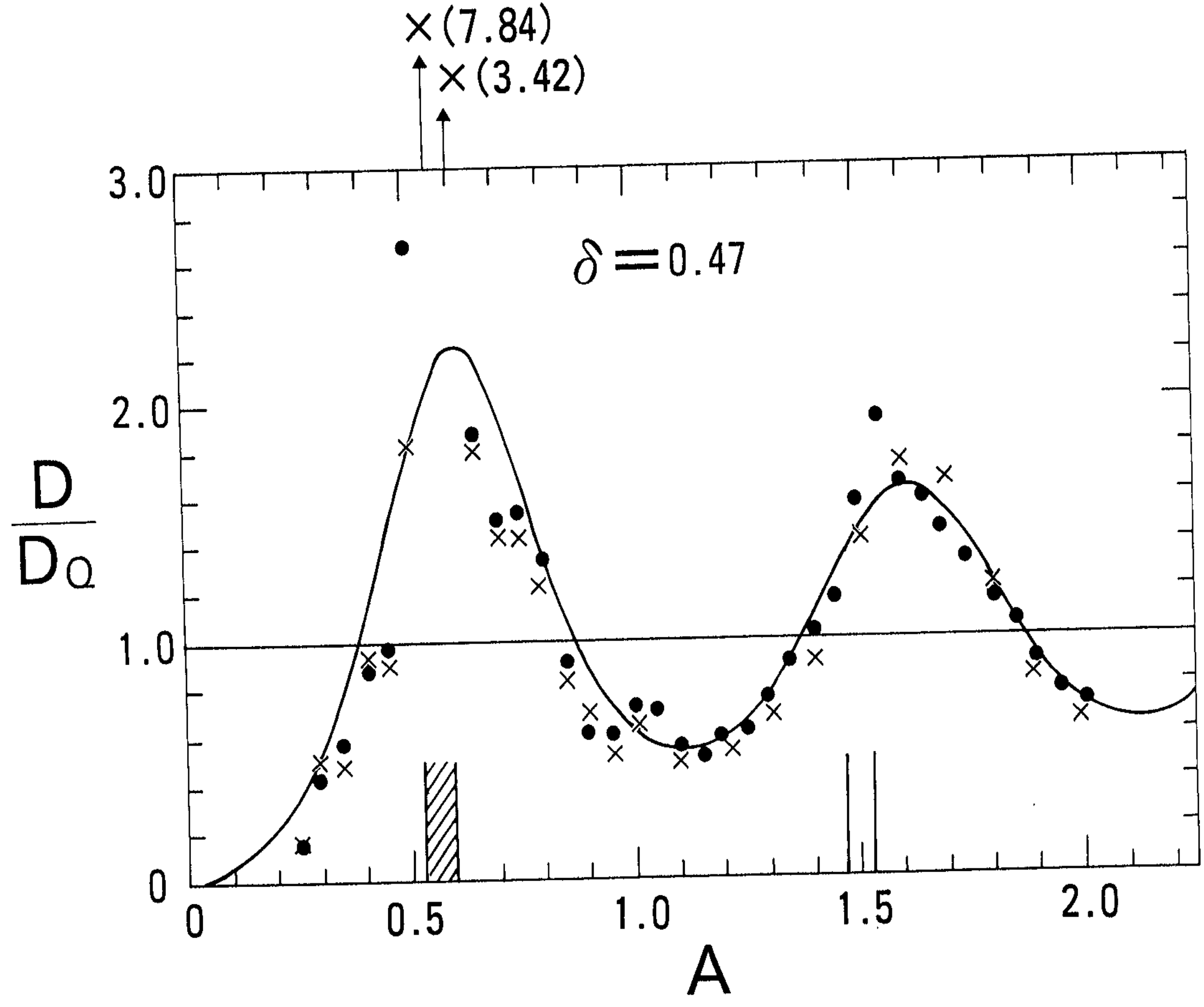

Fig.1

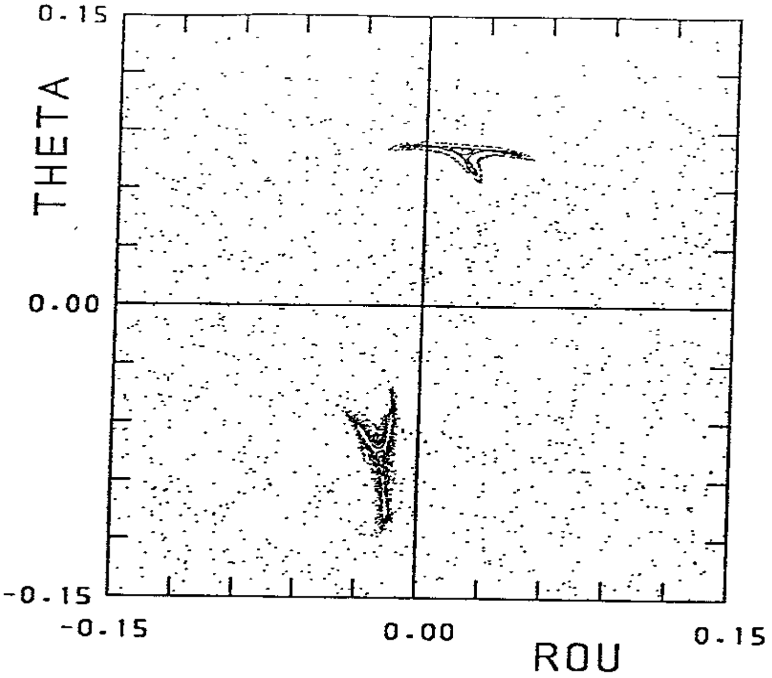
0.15
THETA
0.00
-0.15
-0.15
0.00
0.15
ROU

Fig. 2

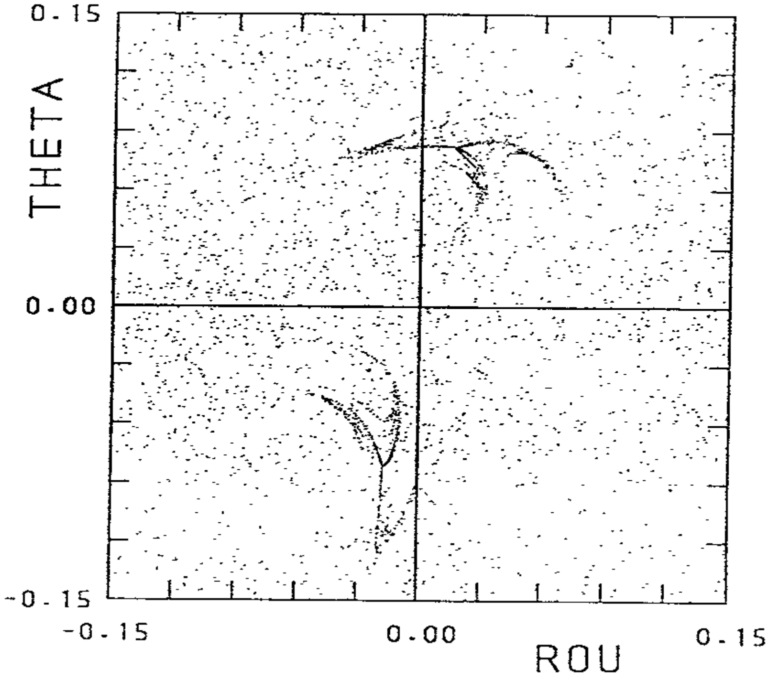
0.15
THETA
0.00
-0.15
-0.15
0.00
0.15
ROU

Fig. 3

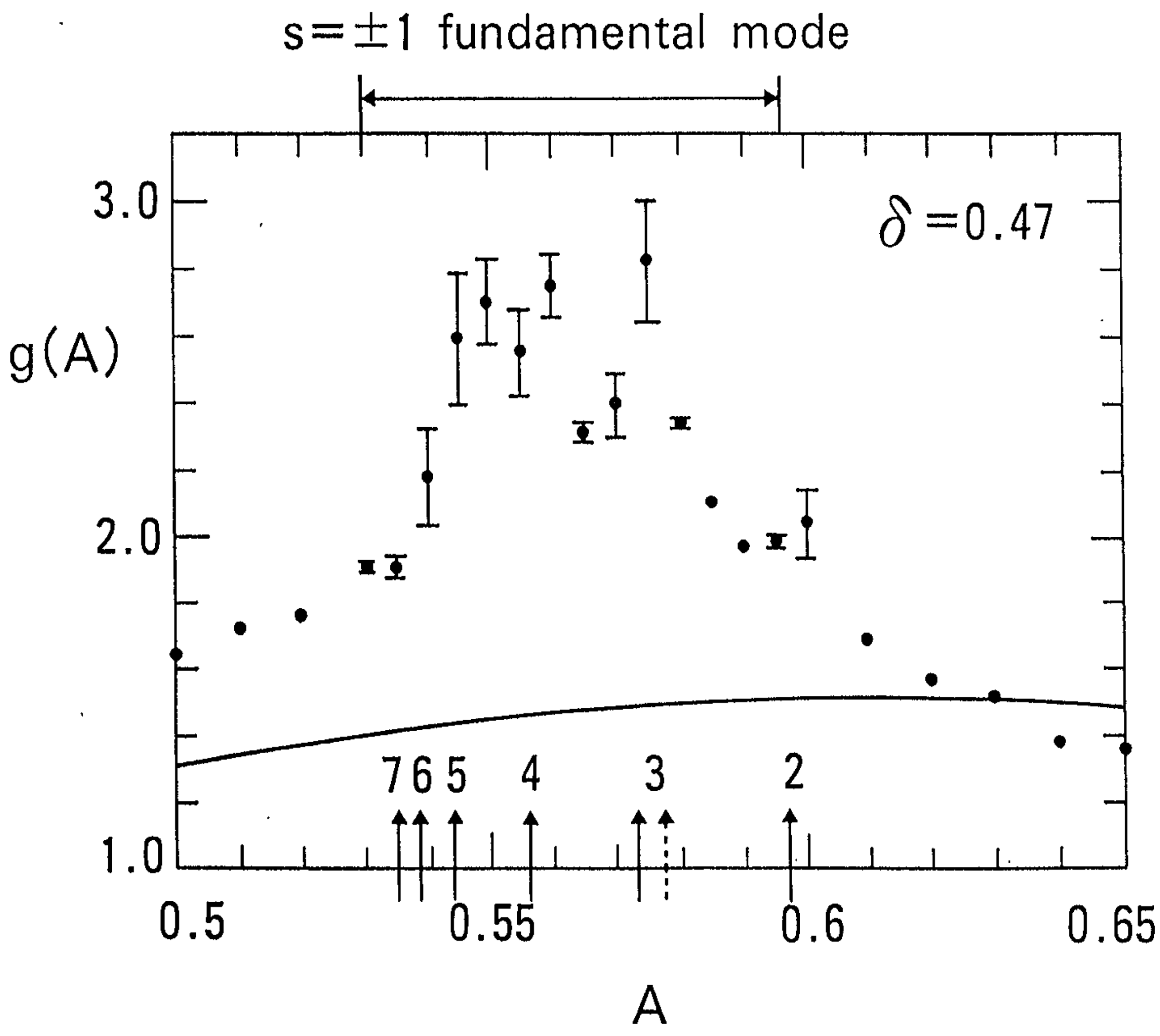

Fig. 4